




Article

# Acceleration Analysis of Canned Motors for SMR Coolant Pumps

Timothy Ngumbi Kanyolo , Harold Chisano Oyando  and Choong-koo Chang \* 

Department of Nuclear Power Plant Engineering, KEPCO International Nuclear Graduate School (KINGS), 658-91 Haemaji-ro, Seosang-myeon, Ulju-gun, Ulsan 45014, Republic of Korea

\* Correspondence: ckchang@kings.ac.kr; Tel.: +82-52-712-7303

**Abstract:** An SMR (small modular reactor) is expected to be able to operate flexibly in conjunction with a high renewable energy penetration grid as a result of improved safety and easy power control compared to large nuclear power plants. SMRs, such as South Korea's System-integrated Modular Advanced Reactor (SMART), are designed to use canned motors (CMs) for their reactor coolant pumps (RCPs) to enhance their safety. CMs passively enhance the reactor's safety by preventing the leakage of radioactive reactor coolant. However, with motor sizes designed to be as small as possible, and the increased air gap of CMs between the stator and rotor, the starting torque may be insufficiently low compared to that of similar-sized induction motors (IMs). Thus, CMs may require variable frequency drives (VFDs) to start. This paper compares the torque characteristics of CMs with those of IMs for SMART's RCPs. ETAP is then used to perform a motor-starting analysis for CMs activated with and without VFDs. The results are presented and analyzed to find out if VFDs can deal with the CM starting torque issue.

**Keywords:** motor acceleration study; reactor coolant pump (RCP); canned motors; small modular reactor (SMR); variable frequency drive (VFD)



**Citation:** Kanyolo, T.N.; Oyando, H.C.; Chang, C.-k. Acceleration Analysis of Canned Motors for SMR Coolant Pumps. *Energies* **2023**, *16*, 5733. <https://doi.org/10.3390/en16155733>

Academic Editors: Loránd Szabó and Feng Chai

Received: 5 July 2023

Revised: 21 July 2023

Accepted: 29 July 2023

Published: 1 August 2023



**Copyright:** © 2023 by the authors. Licensee MDPI, Basel, Switzerland. This article is an open access article distributed under the terms and conditions of the Creative Commons Attribution (CC BY) license (<https://creativecommons.org/licenses/by/4.0/>).

## 1. Introduction

There is a recent increased interest in small modular reactors (SMRs) as a result of their lower initial capital investment compared to larger nuclear power plants (NPPs) and the increase in high renewable energy penetrated grids. SMRs offer small capacity, modularity, and load capabilities [1]. Similar to most modern industrial systems, motors, particularly IMs, dominate an NPP's load capacity [2]. Generally, for pressurized water reactors, reactor coolant pump (RCP) motors have the largest capacities. For enhanced safety, a good number of new SMR designs, such as KAERI's System-integrated Modular Advanced Reactor (SMART), use passive safety systems [3], including CMs in their RCPs [4,5].

In the design of small modular reactors (SMRs), the key objective is to achieve inherent advantages, including enhanced safety, modularity, and reduced construction costs. As part of this design goal, the reactor coolant pump (RCP) and motor size must be as small as possible while still meeting the required operational and safety standards. However, one of the challenges of using canned motor technology for RCPs in SMRs is the larger air gap between the motor stator and rotor compared to similar-sized general motors. While this larger air gap allows for more cooling due to increased coolant flow, it can also result in reduced electromagnetic interlinkage between the stator and rotor fields, leading to less torque [6]. Consequently, CMs might require a larger size to produce the same starting torque as a general induction motor due to their construction.

Nonetheless, the use of variable frequency drives (VFDs) can provide a solution to this issue. VFDs allow for a smoother motor start and precise control over the torque output, which can help optimize the motor's size while still providing the necessary starting torque [7].

To further investigate the torque characteristics and to find ways to satisfy the two conflicting conditions described above, this paper conducts torque comparisons between general IMs and CMs. Additionally, motor-starting studies are performed to compare IM RCPs with CM RCPs and also to compare VFD-driven CM RCPs with CM RCPs started across the line.

To achieve the abovementioned aims, an SMR auxiliary power system (APS) is modeled in an electrical transient analyzer program (ETAP) pegged on the SMART SMR with RCP CMs.

## 2. Literature Review

### 2.1. Induction and Canned Motors

IMs work by electromagnetic induction. The interaction between the three-phase AC-supply connected stator windings' and rotor windings' electromagnetic fields produces slip according to Faraday's Law and the Lorentz force on a conductor. The most common type, the squirrel cage induction motor (SCIM), has a rotor made of conducting bars short-circuited at the ends.

The canned motor (CM) was invented in 1913 and became popular in the 1950s [8] when circumstances in the chemical and nuclear industry favored the seal-less, leak-free operations of centrifugal pumps. A CM combines and hermetically seals a centrifugal pump with an SCIM using two cans placed inside an air gap: on the stator and rotor sides, respectively, as shown in Figure 1 [9]. This leakage prevention property is immensely useful in SMRs since the CM drives RCPs that circulate radioactive reactor coolant. However, due to manufacturing limitations, the cans are made of a bulk metal material instead of laminations and this introduces eddy current losses that, in turn, interact with the air gap's magnetic field, an effect called magnetic shielding [10].

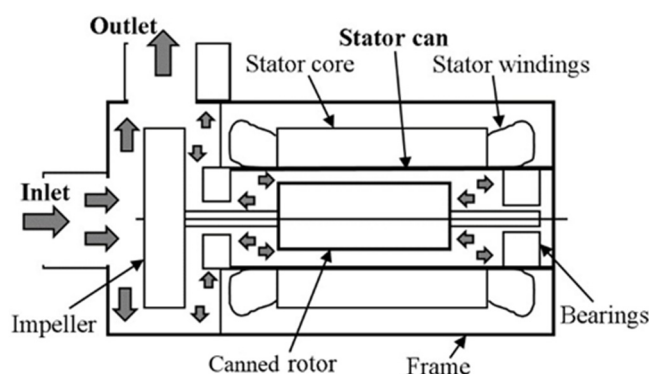


**Figure 1.** Outline of a canned motor.

### 2.2. Motor Torque Characteristics

Connecting a three-phase supply to the SCIM stator produces a rotating magnetic field (RMF) that cuts across the short-circuited rotor cage bars inducing a voltage that causes a high current flow. The current interacts with the stator's field to produce a torque that drags the rotor along the path of the RMF. Figure 2 shows a typical IM torque speed curve [7]. Notably, the torque developed at zero speed is the starting or locked rotor torque (LRT), while the one required to run a full load at a rated speed is the full load torque (FLT). In between, the maximum and minimum torques are pull-up (PUT) and breakdown torques (BDT), respectively.

The RCP motor's load torque is typical for a centrifugal pump, i.e., it follows the square law. The accelerating torque, i.e., difference between the motor torque and load torque curves, accelerates the motor to its operating speed and within its thermal limits [7]. Insufficient acceleration torque may lead to the motor overheating causing motor stator winding damage. The motor may also stall and draw high currents that may damage other motors or loads connected to the same or nearby buses.

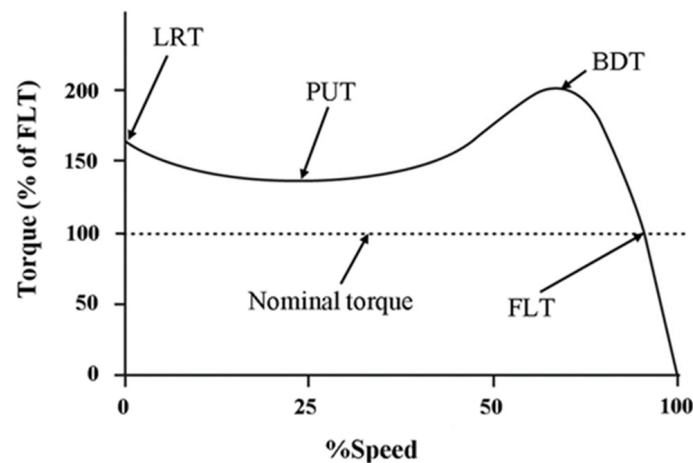


Figure 2. Typical induction motor torque–speed curve.

The CM’s electromagnetic design affects eddy current losses and highly depends on air gap and can thickness. There are three factors considered in the size determination of the air gap between the cans [11]. Firstly, the clearance needs to be as small as possible such that the starting torque and the efficiency of electromagnetic conversion satisfy the pump requirements. The other two factors involve having the clearance as wide as possible to guarantee the motor cooling performance and also large enough to maintain rotor system stability.

According to studies [12], and as shown in Figure 3, the addition of cans to an IM decreases the magnetizing current ( $I_{oc} < I_o$ ) resulting from increased magnetizing inductance ( $L_{mc} > L_m$ ) and decreased magnetizing resistance ( $r_{mc} < r_m$ ). Conversely, an increased slot leakage flux causes a corresponding increased stator ( $I_{1c} > I_1$ ) and rotor ( $I_{2c} > I_2$ ) leakage inductance. Overall, the effect is a lower power factor (PF), efficiency, and starting torque [6,10]. Stator ( $r_1$ ) and rotor ( $r_2$ ) resistances are mainly unchanged.

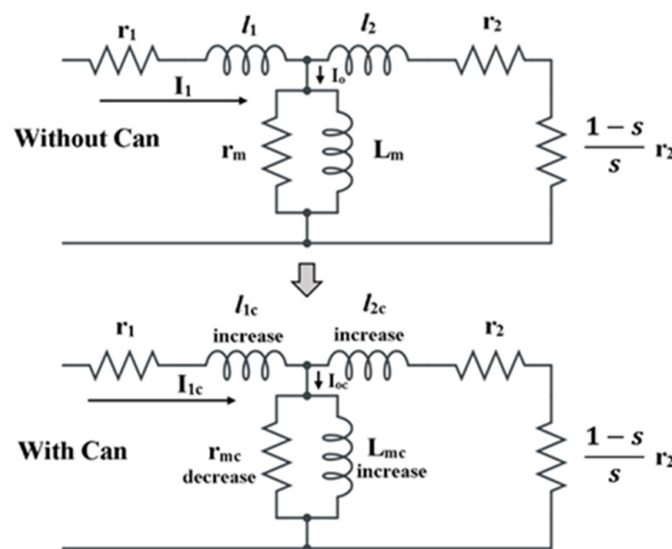


Figure 3. Equivalent circuit variation: IM vs. CM.

The usual efficiency of a CM is 50% to 70%, PF is 80%, and BDT higher than 200% of FLT. Studies [13] showed that these parameters were higher for larger-capacity CMs. A 1.9 kW CM was, for instance, shown to have a locked rotor torque that was 92.2%, that of a same-sized IM [14]. Figure 4 shows typical NEMA design letter A or B torque–speed curves for an IM and the relative curve for a similar-sized CM, i.e., CM with lower LRT and BDT values.

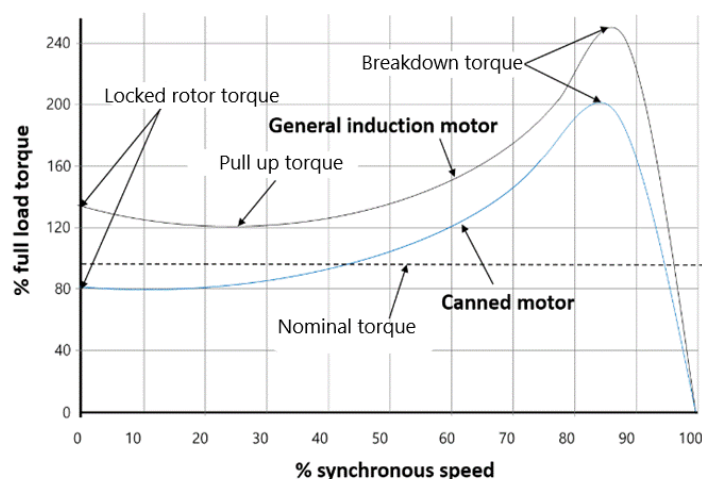


Figure 4. Relative torque–speed curve: IM vs. CM.

### 3. Methodology

#### 3.1. Selection of Motor-Starting Method for Canned Motor RCP

In general, three-phase IMs of power plants are self-starting. However, a starter may be required in order to reduce the inrush current to the machine that can be as high as five to seven times the full load current (FLC) and provide overload protection. The starter method depends on various factors, such as allowable voltage drops, inrush current limitations, torque, acceleration time, cost, and compliance with standards, such as IEEE 3002.7. The major commercially used starting methods are full voltage-fixed frequency (direct online or across the line), reduced voltage-fixed frequency (wye-delta, autotransformer, and soft starter), and variable frequency drive (VFD) starts.

Across-the-line starting (direct online) is used by default. If there is a need to limit the inrush current or starting torque, reduced voltage-starting is then used.

On the other hand, variable frequency drives (VFDs) convert a fixed voltage and frequency input into a variable voltage and frequency output using power electronics. The most common VFD, the PWM-type, improves stable voltage and frequency outputs and eliminates cogging in motors [15]. A constant voltage-to-frequency (volts-per-hertz) ratio leads to a fixed flux. If the volts-per-hertz ratio is based on the rated voltage and rated frequency, and kept constant by the use of a VFD, then it follows that the rated flux and rated motor torque are maintained without the risk of magnetic core saturation. The motor thus achieves a rated torque at a rated speed with a constant rated motor flux [16]. This speed and torque control is a great advantage over the other reduced voltage-fixed frequency methods.

The main issue with the canned motor RCP is its low-torque development as a result of the smaller size of the motor (relative to larger NPPs) and the motor characteristics of a canned motor. This is particularly important when starting the motor because the voltage drop across the nearest buses (as a result of the inrush currents) is the highest. If the motor takes too long to start due to a low developed motor torque, the motor insulation may be damaged for exceeding its thermal limits and the suppressed and sustained low voltage may stall other running motors in the same system. Even though full torque can be provided by both across-the-line and VFD starts, the VFD start has the added benefit of limiting the starting current, which is the most crucial given that the RCP motor has the largest load in the SMR and thus causes the greatest voltage drops. The other benefit of using a VFD with the RCP is that it also eliminates the need for an anti-reverse rotation system [17]. The other methods (reduced voltage-fixed frequency starts) are also able to limit inrush currents but at the expense of the important torque development in the motor. This paper thus proposed the use of a VFD to start CMs, and therefore focused on direct online (DOL) and VFD starts.

However, introducing a VFD start as a motor driving method also introduced challenges [15,18,19]. Electromagnetic emissions can be produced from the VFD's output terminal and cause an interference. This can be mitigated by proper specifications, using shielded power cables to connect the VFD or using mitigation devices, such as electromagnetic interference (EMI) filters and common-mode chokes. Another issue is that of the harmonics produced by the power electronics that comprise the VFD and that have a negative impact on PF and other electronic equipment. Using adequate filtering to smoothen the input current can mitigate this and reduce the overall current harmonic distortion. Additionally, PWM pulse build-up can break down motor insulation and stress the windings, and, to mitigate the insulation damage, the motor terminal voltage can be lowered by using line reactors, resistor–capacitor snubbers, and resistor–inductor–capacitor (RLC) low-pass filters. The other challenges associated with the use of VFDs are acoustic noises produced by VFDs resonating with the system at certain speeds that shortens the life of the VFD and connected motor, high initial investment costs due to VFD complexity, and the need for reliability studies as a result of the increased failure chance of solid-state components of the VFD.

### 3.2. Motor-Starting Simulation Using ETAP

In order to perform this study, the SMR's auxiliary power system (APS) was designed considering physical separation, redundancy, independence, and diversity criteria. The chosen configuration is shown in the conceptual diagram in Figure 5. Additionally, and in order to compare the motor-starting performances of general induction motor RCPs with canned motor RCPs, the SMR's APS design was then summarized and modelled on ETAP as per Figure 6. This was performed because the focus of the study involved studying motor-starting and determining of motor-starting times and motor-starting torques.

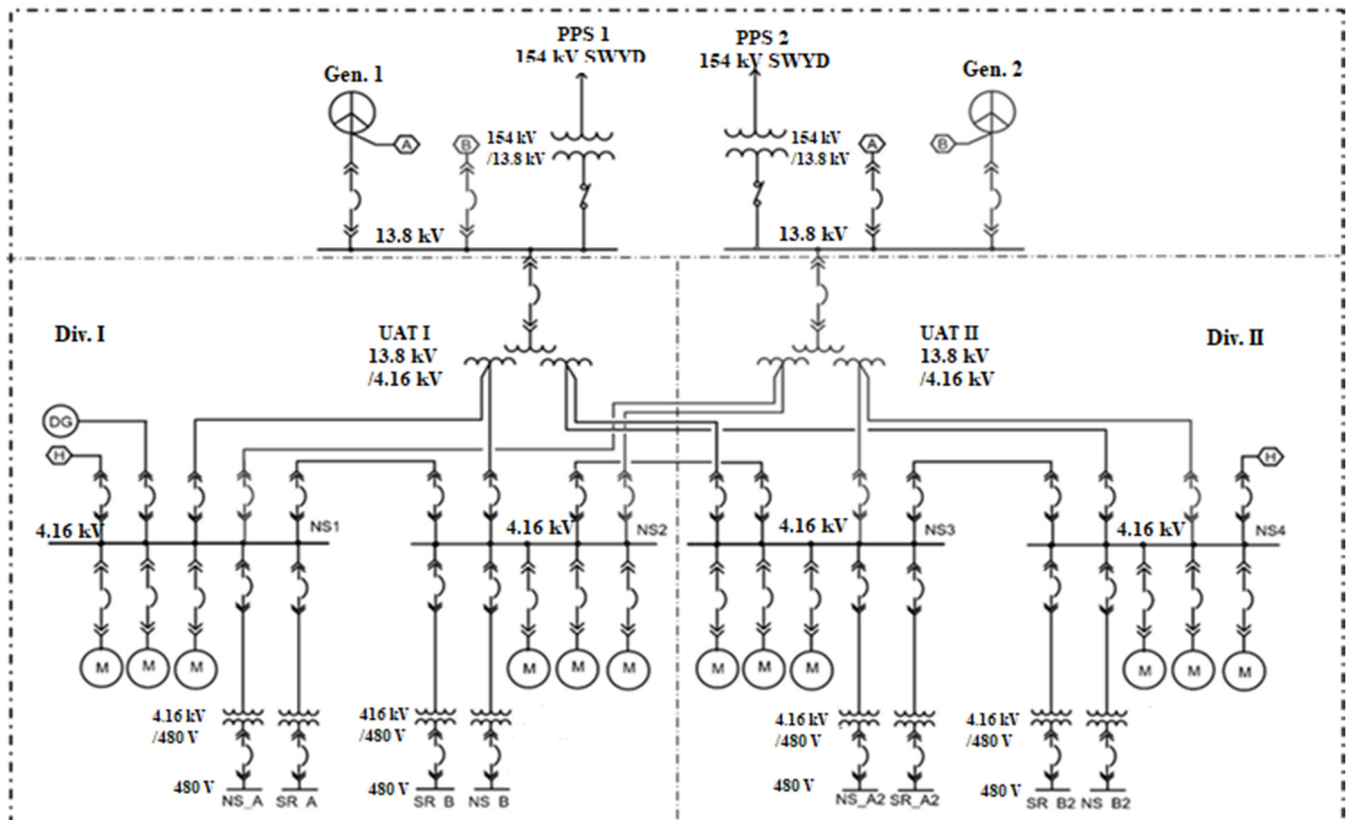


Figure 5. Concept diagram for auxiliary power system of SMR.

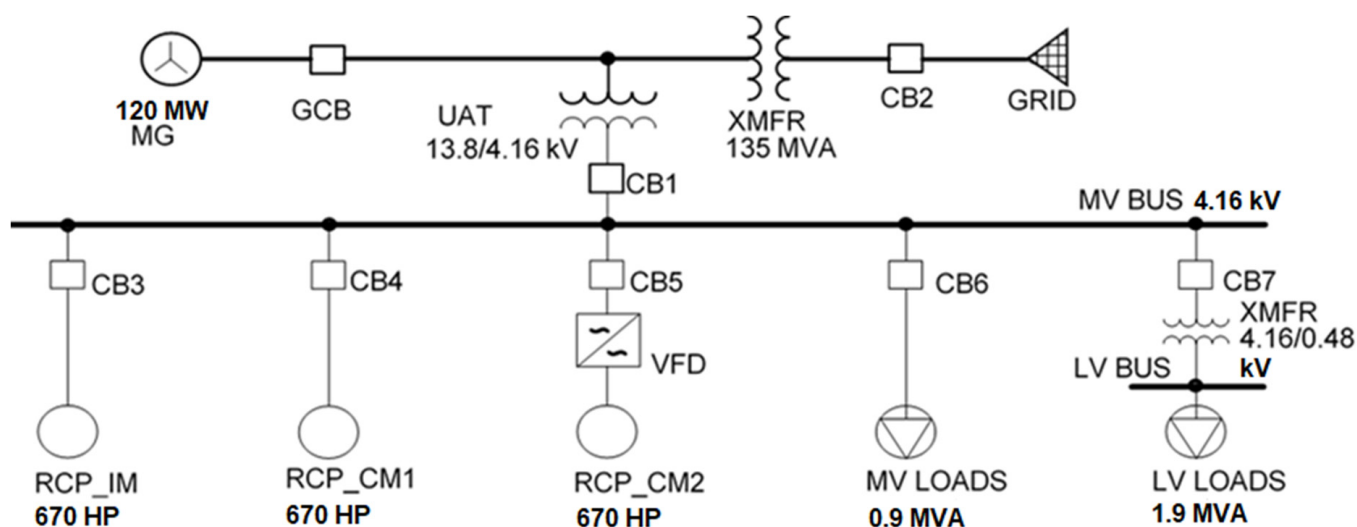


Figure 6. Partial single-line diagram for SMR auxiliary power system.

One 4.16 kV bus was conceived as enough to show voltage drops across the system, while non-RCP loads were lumped. A “Single-Cage Motor IM with deep bars” circuit model in the ETAP library (Table 1) was used to model the IM and CM RCPs by modifying equivalent circuit parameters (stator, rotor, and core inductances). From the literature reviews, the ratio between the CM LRT and that of similar-sized IMs was used as a guide [12].

Table 1. ETAP input data for RCP motors (Settings).

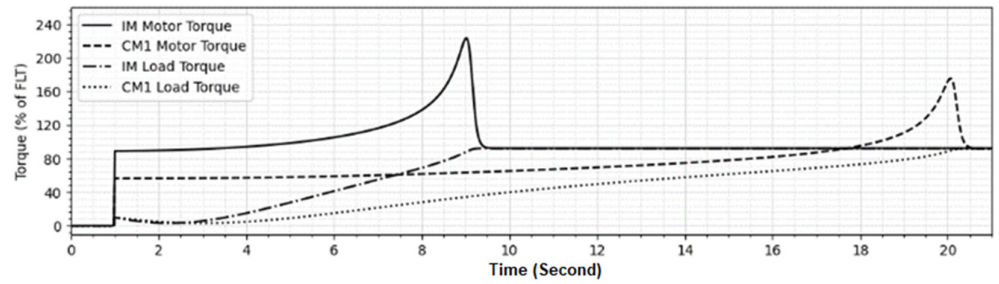
Setting	Induction Motor	Canned Motor
HP (kW)	500	500
Voltage rating (kV)	4	4
Torque max, BDT (%)	220.1	171.87
Locked rotor current (%)	449.92	353.14
Locked rotor torque (%)	90.05	56.48
Locked rotor PF (%)	19.52	15.21
Efficiency (%)	97.87	97.61
Full load PF (%)	92.80	91.08
Circuit design class	HV-HS-HT	HV-HS-HT
Circuit model	Estimated	Estimated

#### 4. Results and Discussion

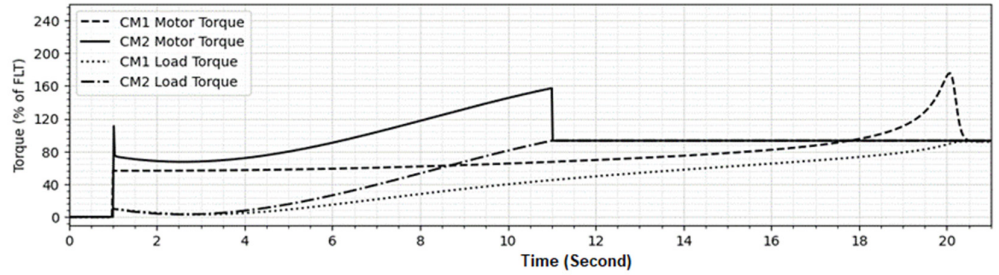
The study captured the comparison of direct online (DOL) starting one IM (IM), DOL starting one CM (CM1), and a variable frequency drive (VFD) starting a second CM (CM2). The total simulation time was twenty-one seconds. The results of the motor-starting study are shown in Figure 7a–e, discussed thereafter, and summarized in Table 2.

Table 2. ETAP input data for the RCP motors (settings).

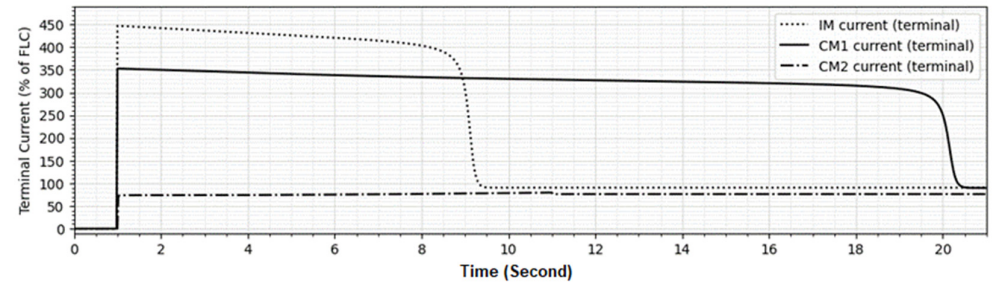
Setting	DOL IM	DOL CM1	VFD CM2
Start-up time (s)	8.7	19.7	10
Locked rotor torque developed (% FLT)	88.9	56.3	110.8
Locked rotor acceleration torque (% FLT)	78.9	46.3	100.8
Maximum current (% FLC)	446.9	352.7	79.4
Bus voltage before motor start (% nominal kv)	98.1	98.1	97.9
Maximum voltage dip (% bus nominal kv)	2.6	2.1	0.2
Minimum bus voltage (% nominal kv)	95.5	96.0	97.7



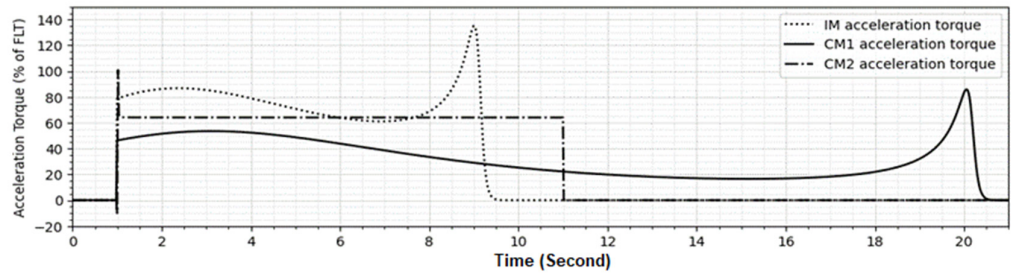
(a)



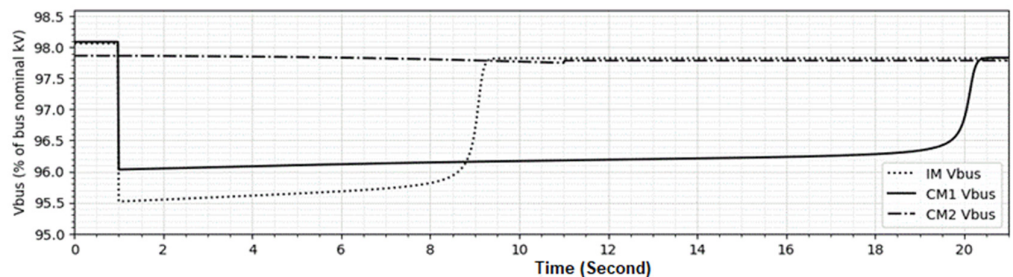
(b)



(c)



(d)



(e)

**Figure 7.** RCP motor-starting results for IM, CM1, and CM2. (a) Motor and load torques (IM/CM1) vs. starting time. (b) Motor and load torques (CM1/CM2) vs. starting time. (c) Motor-starting current (IM/CM) vs. starting time. (d) Motor acceleration torque (IM/CM) vs. starting time. (e) Bus voltage (IM/CM) vs. starting time.

The DOL-started IM (IM) achieved a full load torque and rated speed of 8.7 s after starting compared to the DOL-started CM (CM1) that took 19.7 s. The VFD-started CM (CM2), however, achieved a full load torque and rated speed at 10 s, compared to 19.7 s for the direct online-started CM1 (CM1).

Rated torque was achieved rapidly by the direct online-started IM (IM) compared to the direct online-started CM (CM1). This was because, even though the load torques were similar, the IM had a higher starting torque resulting in a higher accelerating torque and shorter accelerating time. The reduced starting torque of CM1 was mainly caused by eddy current losses in the canned motors. Additionally, even though both direct online-started CM (CM1) and VFD-started CM (CM2) should have had the same starting torques, employing the VFD starter resulted in a higher developed torque (almost full load torque) at the start for CM2. This was because the VFD could utilize a V/Hz control scheme to achieve a constant flux at reduced motor voltages. Consequently, for the same load torque, CM2 had a higher resultant acceleration torque compared to CM1, thus achieving a faster rated torque. All the results are illustrated in Figure 7a–c.

The bus percentage voltage drops were similar for the direct online-started IM (IM) and CM (CM1); however, the IM had a slightly greater drop (i.e., the bus voltage decreased from a 98.1% bus nominal kV to 95.5%, a difference of 2.6%) compared to CM1's (decrease from a 98.1% bus nominal kV to 96.0% bus nominal kV, a difference of 2.1%). Additionally, as shown in Figure 7d, there is a significant difference in the voltage drops for the direct online-started CM (CM1) and VFD-started CM (CM2). CM2 had no discernible voltage drop compared to CM1, i.e., CM2 bus voltage drops from a 97.9% bus nominal kV to 97.7% bus nominal kV, a difference of only 0.2%. The difference in voltage drops was attributed to IM's higher line current (inrush current of up to 446% of full load amps) compared to CM1 (352.7% of full load current) and CM2 (a maximum of 79.4% full load current), while the VFD significantly reduced the voltage drop with barely any inrush current to the motor. The VFD achieved this due to the reduced voltage applied to the motor at the start. However, even though CM1 has a lower maximum current compared to IM, the duration of its inrush current is longer and care may need to be taken to ensure the motor does not exceed its thermal limits. The inrush currents are shown in Figure 7c.

Most of the SMRs in the recent development rush around the world are adopting CMs for RCP pumps [5]. The reason for the canned motor is to increase safety by preventing coolant leakage from the motor shaft. On the other hand, due to its structural characteristics, the starting torque of a canned motor is lower than that of an IM of the same size, which means that the size of the motor must be increased to obtain the desired torque. However, since the size of the entire module must be minimized for the SMR to be manufactured as a modular type, the size of the RCP motor must also be minimized. It is necessary to take measures to handle both of these conflicting conditions.

If this problem is overlooked during the SMR development stage, the production and construction of SMRs will be greatly disrupted. The results of the study show that installing a VFD for canned motor-starting is a valid countermeasure, i.e., the operation characteristics of the same size canned motor exceed the operation characteristics of the IM motor.

## 5. Conclusions

In recent years, SMRs have emerged as a way to address carbon net zero. As such, more than 70 SMR models are reportedly under development worldwide [5]. In order to secure greater nuclear safety of SMR, canned motors are being adopted to drive RCP pumps. However, few auxiliary power system designs have been confirmed or proposed to include canned motor driving.

In this paper, a power system design of a two-module SMR was presented to help design the electric power system of an SMR, and based on this, an optimum motor drive system was selected and its technical feasibility was demonstrated through simulations.



The major motor in the SMR system is an RCP. However, a challenge was introduced: the smaller size of the motors due to the lower loads of the SMR meant that the motors produced lower torques. Additionally, in a bid to enhance the safety of the SMR, SMR RCPs use CMs to prevent the leakage of radioactive coolant. The low torque, as a result of these challenges, increased the risk of the RCP motor not starting or even stalling. Furthermore, SMRs are expected to perform load following to cope with variable energy sources, which means that RCPs may be required to start and stop more frequently compared to base-load nuclear power plants. Therefore, the selection of the motor-starting method was important. This study proposed using VFD-starting as a suitable motor-driving method to overcome low-torque issue. The solution also solved other challenges, such as starting the motors easily to reduce mechanical shock and increase their lifetime. However, surge protection measures must be taken as the VFD may cause voltage surges and damage to the motor.

CMs, compared to similar-sized IMs, were shown through ETAP simulations to have a reduced inrush current compared to similar-sized IMs. Further simulations showed that VFD-starts overcame the reduced starting torque issue of the CMs, thereby improving the starting torque from around 46.3% of the full load torque to 100.8% of the full load torque. In addition to this, the starting times were reduced due to the higher motor torque developed that was sufficient to guarantee starting. The paper therefore concluded that the VFD-starting of SMART SMR's RCP CMs was a viable solution to the low-starting-torque problem associated with CMs.

Further study is required to determine if additional VFD-associated costs can be justified in the long run and if the introduced electromagnetic emissions and harmonics would be within the allowable limits.

**Author Contributions:** T.N.K. performed the simulation and wrote this paper as the first author. H.C.O. designed the auxiliary power system of the SMR as the second author. C.-k.C. guided the design and analysis as a corresponding author. All authors have read and agreed to the published version of the manuscript.

**Funding:** This research received no external funding.

**Data Availability Statement:** Data is unavailable due to ethical restrictions.

**Acknowledgments:** This research was supported by the 2023 Research Fund of the KEPSCO International Nuclear Graduate School (KINGS), Ulsan, Republic of Korea.

**Conflicts of Interest:** The authors declare no conflict of interest.

## References

1. Chang, C.; Oyando, H.C. Review of the Requirements for Load Following of Small Modular Reactors. *Energies* **2022**, *15*, 6327. [[CrossRef](#)]
2. Villaran, M.; Subudhi, M. *Aging Assessment of Large Electric Motors in Nuclear Power Plants*; Nuclear Regulatory Commission: New York, NY, USA, 1996.
3. Bae, K.H.; Kim, S.D.; Lee, Y.; Lee, G.H.; An, S.; Lim, S.W.; Kim, Y.I. Enhanced safety characteristics of SMART100 adopting passive safety systems. *Nucl. Eng. Des.* **2021**, *379*, 111247. [[CrossRef](#)]
4. Carelli, M.D.; Ingersoll, D.T. *Handbook of Small Modular Nuclear Reactors: Second Edition*; Woodhead Publishing: Duxford, UK, 2020.
5. IAEA. *Advances in Small Modular Reactor Technology Developments—A Supplement to: IAEA Advanced Reactors Information System (ARIS)*; IAEA: Vienna, Austria, 2020.
6. Hu, X.; Li, Y.; Luo, L. The Influence of Air Gap Thickness between the Stator and Rotor on Nuclear Main Pump. *Energy Procedia* **2017**, *142*, 259–264. [[CrossRef](#)]
7. IEEE. *3002.7-2018—IEEE Recommended Practice for Conducting Motor-Starting Studies and Analysis of Industrial and Commercial Power Systems*; IEEE: New York, NY, USA, 2019.
8. Neumaier, R. *Hermetic Pumps: The Latest Innovations and Industrial Applications of Sealless Pumps*, 1st ed.; Gulf Professional Publishing: Woburn, MA, USA, 1997.
9. Weili, L.; Xiaochen, Z.; Wenbiao, C.; Junci, C. *Numerical Analysis of Thermal Behavior of Canned Motor*; IEEE: New York, NY, USA, 2007.
10. Hu, K.; Zhuang, H.; Yu, Q. Electromagnetic Shielding Effect of a Canned Permanent Magnet Motor. *Energies* **2020**, *13*, 4666. [[CrossRef](#)]

11. Xu, R.; Song, Y.; Gu, X.; Lin, B.; Wang, D. Research on the clearance flow between stator and rotor cans in canned motor RCP. *Ann. Nucl. Energy* **2021**, *164*, 108583. [[CrossRef](#)]
12. Yamazaki, K. Modeling and Analysis of Canned Motors for Hermetic Compressors Using Combination of 2D and 3D Finite Element Method. In Proceedings of the International Electric Machines and Drives Conference, ICEM, Seattle, WA, USA, 9–12 May 1999; p. 337.
13. Wang, Y.; Yao, Z.; Shen, H.; Xue, Y.; Cheng, D. Modeling and Analysis of Canned Motor of the Nuclear Reactor Coolant Pump. *Appl. Mech. Mater.* **2013**, *328*, 955–959. [[CrossRef](#)]
14. Yuejun, A.; Zhiheng, Z.; Ming, L.; Guangyu, W.; Xiangling, K.; Zaihang, L. Influence of asymmetrical stator axes on the electromagnetic field and driving characteristics of canned induction motor. *IET Electr. Power Appl.* **2019**, *13*, 1229–1239. [[CrossRef](#)]
15. Blair, T.H. Variable Frequency Drive Systems. In *Energy Production Systems Engineering*; The Institute of Electrical and Electronic Engineers: New York, NY, USA, 2016. [[CrossRef](#)]
16. Vandermeulen, A.H.; Natali, T.J.; Dionise, T.J.; Paradiso, G.; Ameen, K. Exploring New and Conventional Starting Methods of Large Medium-Voltage Induction Motors on Limited kVA Sources. *IEEE Trans. Ind. Appl.* **2019**, *55*, 5. [[CrossRef](#)]
17. Park, J.; Field, R.M.; Kim, T.-R. Study on the VFD (Variable Frequency Drive) for RCP (Reactor Coolant Pump) Motors of APR1400. In Proceedings of the Transactions of the Korean Nuclear Society Autumn Meeting, Pyeongchang, Republic of Korea, 30–31 October 2014.
18. Moncrief, W. *Guide to the Industrial Application of Motors and Variable-Speed Drives*; Report No. 1005983; EPRI PEAC Corporation: Palo Alto, CA, USA, 2001.
19. Khan, S. *Industrial Power Systems*; CRC Press, Inc.: Boca Raton, FL, USA, 2007. [[CrossRef](#)]

**Disclaimer/Publisher's Note:** The statements, opinions and data contained in all publications are solely those of the individual author(s) and contributor(s) and not of MDPI and/or the editor(s). MDPI and/or the editor(s) disclaim responsibility for any injury to people or property resulting from any ideas, methods, instructions or products referred to in the content.